Fashion and Textiles

3D-printed thermoplastic polyurethane for wearable breast hyperthermia

Yusuke Mukai[1], Sixian Li[1] and Minyoung Suh[2]*

*Correspondence:
msuh2@ncsu.edu
[2] Associate Professor,
Department of Textile
and Apparel, Technology
and Management, North
Carolina State University,
1020 Main Campus Drive,
Raleigh, NC 27606, USA
Full list of author information
is available at the end of the
article

Abstract

Microwave breast hyperthermia is a class of cancer treatment, where breast temperature is elevated by a focused electromagnetic (EM) radiation to impair cancer cells. While the current mainstream in microwave breast hyperthermia is centered on bulky and rigid systems, wearable antennas would offer considerable benefits such as superior conformity to individual patient anatomy and better comfort. In this proposition, this paper presents 3D-printed flexible antenna prototypes for wearable breast hyperthermia applications. Since the dielectric properties are expected to dominate the antenna gain but could be influenced by the solid volume percentage, this work first investigates the relationship between the dielectric properties and solid volume percentage of a 3D-printed flexible filament. From this, it is found that with decrease in the solid volume percentage, the dielectric constant decreases following the classic theory of dielectric mixture. Based on this observation, optimal antennas are designed for substrates in different infill levels by running a 3D full-wave EM simulator and fabricated by 3D printing a polyurethane filament. Temperature elevations in a synthetic breast tissue are measured by a thermometer and are ~ 5.5 °C and ~ 3.2 °C at the 5 mm- and 7 mm-deep locations, respectively. The infill percentage makes little difference in the heating efficacy. Based on these findings, this translational study sheds light on the possibility of wearable breast hyperthermia with the 3D-printed flexible and conformal antennas.

Keywords: Wearable technology, Permittivity, Conformal antenna design, Breast hyperthermia, Additive manufacturing

Introduction

Treatment of breast cancer is one of the key research topics in health sciences, and as a non-invasive technique, microwave hyperthermia has recently been spotlighted (Anghileri & Robert 2019; Curto et al. 2018; Mukai 2016; Pang & Lee 2016). In microwave hyperthermia, the body temperature is locally or regionally raised to 39–45 °C by a focused electromagnetic (EM) radiation or microwave. The consequential biological effects include changes in the local blood flow, thermal damage and cellular death, induced by changes in the local oxygenation and pH (Mukai & Suh 2019b; Peng et al. 2016).

The current mainstream in microwave hyperthermia research focuses primarily on the bulky and heavy antennas, which would impose considerable discomfort to patients

Mukai *et al. Fash Text*   (2021) 8:24

Page 2 of 12

during treatment (Curto et al. 2018). As a more patient friendly and pervasive option, wearable antennas have recently been proposed for hyperthermia applications, and those include water bolus (Curto et al. 2015, 2018; Curto & Prakash 2015) and textile antennas (Mukai 2019; Mukai & Suh 2018, 2019b, 2020). Having flexible and small form factors, these wearable antennas are claimed to offer substantial benefits such as superior conformity to individual patient anatomy and better comfort (Curto et al. 2015, 2018; Mukai 2019; Ramasamy et al. 2015).

Although these approaches are auspicious, there are several challenges. For instance, the antennas with water boluses require a relatively heavy water-circulating system for cooling (Curto et al. 2018), which would deteriorate the wearability and comfort (Mukai & Suh 2020). Textile antennas, on the other hand, seem to be more propitious since conventional textile-like feel is an attractive feature to wearable applications in contact with skin. However, the fabrication of textile antennas largely relies on the manual labor (Locher et al. 2006; Mukai 2019; Mukai & Suh 2020), and consequently, handmade production to meet individual needs would be unrealistic in terms of production cost and efficiency.

3D-printed antennas (Bjorgaard et al. 2018; Liang et al. 2016) could be a great alternative. In 3D printing, molten resin is deposited layer-by-layer to build an antenna structure. It is not an instantaneous task and takes time to 3D-print. However, compared to the traditional fabrication of a textile product, 3D printing enables accurate and rapid manufacturing of custom designs at low cost, which is essential for successful production (Noorani 2017). In addition, with the use of flexible thermoplastic materials, flexibility and comfort do not have to be sacrificed (Mirzaee et al. 2015), and this would support a long-term and continuous modality of treatment. Furthermore, theoretically unlimited design options enabled by 3D printing (Noorani 2017) could open up the possibility to manipulate the infill (solid volume) percentage of antenna substrate and engineer the dielectric properties for a maximum antenna performance. For instance, increasing the porosity (void fraction) was reported to lower the permittivity of cotton fabrics and hence could improve the antenna gain, bandwidth and efficiency (Mukai 2019; Mukai et al. 2020; Mukai & Suh 2019a). In a similar rationale, Xu et al. (2020) used a spacer fabric that increases the porosity to enhance the antenna performance. These pieces of evidence lead to a premise that reducing the infill percentage of a 3D-printed antenna substrate could lower the permittivity, which in turn permits to build an antenna with a higher heating performance.

In this context, the first objective of this research was to investigate the effect of infill percentage on the dielectric properties of a 3D-printed flexible substrate. Since the dielectric properties dominate the antenna gain but could be influenced by the solid volume percentage, it was crucial to uncover the relationship between the dielectric properties and infill (solid volume) percentages. The second objective was to design and fabricate 3D-printed antennas and investigate the impact of the infill percentage on the heating performance for wearable microwave hyperthermia applications. By using the acquired dielectric property information, antennas were designed for substrates in different infill levels by operating a 3D full-wave EM simulation software and fabricated by 3D printing a flexible filament and placing an adhesive-backed conductive foil. Temperature elevations in breast tissue by these antenna samples were measured, and the effect of the infill

Mukai *et al. Fash Text*   (2021) 8:24

Page 3 of 12

percentage on the heating efficacy was discussed. The possibility of administering micro-wave breast hyperthermia therapy with a 3D-printed antenna was followed.

Methods

Breast phantom

As pointed out in literature (Curto et al. 2018; Mukai 2019; Mukai & Suh 2020; Pang & Lee 2016), the expected treatment (heating) efficacy of a wearable microwave hyper-thermia device critically depends on the biophysical (e.g., perfusion and dielectric) and dimensional (e.g., tumour size and location) characteristics of breasts, but these characteristics differ significantly on an individual basis. For the purpose of model analysis, this work employed a simple homogeneous breast phantom in a hemispheric shape (radius = 50 mm), which was investigated for hyperthermia applications in previous works (Mukai 2019; Mukai & Suh 2018, 2019b, 2020).

This phantom was produced by following previous research (Ito et al. 2001; Mukai 2019; Mukai & Suh 2018). 10.46 g of agar, 3.76 g of sodium chloride, and 0.20 g of sodium azide were completely dissolved in 337.50 g of deionized water. After heating the solution on a stove and reaching the boiling point, the solution was removed from the heat source. To this solution, a mixture of 8.44 g of TX-151 and 33.75 g of polyethylene powder were sprinkled and mixed uniformly. This liquid was then poured into a 3D-printed breast mold and quenched at room temperature to form a hemispheric shape (Fig. 1). The complex permittivity, specific heat and density of this breast phantom were 48.5– 23.28j, 3.63 J/g·K and 900 kg/m^3, respectively (Ito et al. 2001; Zajicek & Vrba 2010).

3D printing

For 3D printing, a dual-head fused deposition modelling (FDM) printer (Luzbot Taz 6) was used. A thermoplastic polyurethane (TPU) filament with a low shore hardness (85A) was supplied by NinjaTek to produce highly flexible structures. For the best print quality, the printing temperature and speed were respectively set to 225 °C and 25 mm/s based on a preliminary investigation (Li 2019).

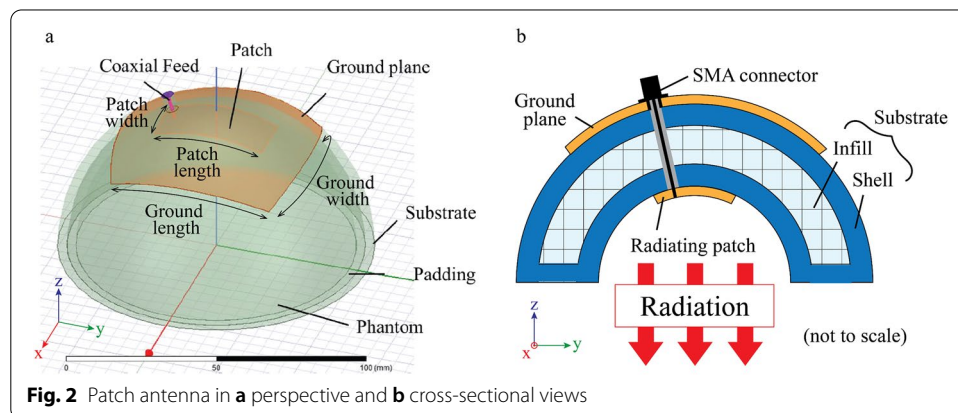**Fig. 1** Homogeneous breast phantom
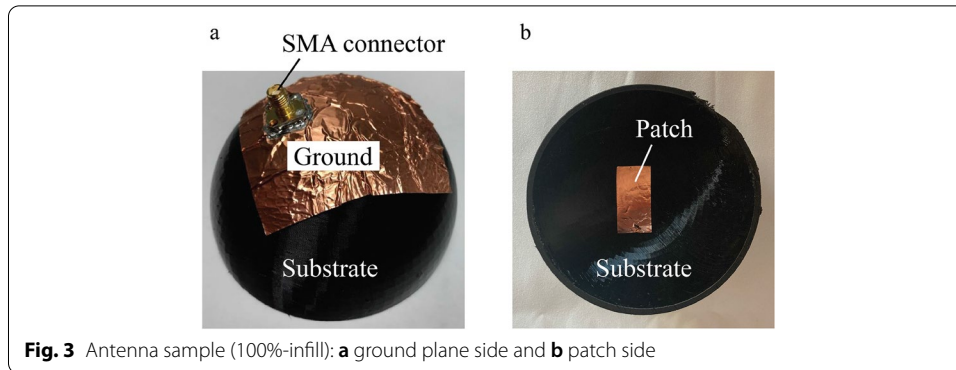
Permittivity measurements

The dielectric properties of 3D-printed TPU were measured in three infill percentages (40%, 70% and 100%) by the resonant cavity method (Bharambe 2016; Mukai et al. 2018) to uncover the effect of the solid volume percentage on the dielectric properties. In brief, a cylindrical cavity made of copper was filled with the 3D-printed TPU, and the resonant frequency for the TM_{010} mode was observed by operating a calibrated vector network analyzer (Agilent E5071C ENA Series Network Analyzer). The dielectric constant (real part of the relative permittivity; ε_r') and the loss factor (imaginary part of the relative permittivity; ε_i') were respectively calculated from the shift in the resonant frequency and the change in the quality factor by the 3D-printed TPU (Bharambe 2016).
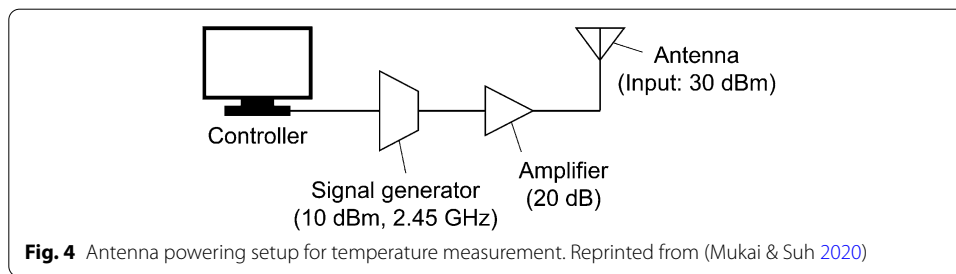
Antenna design & fabrication

In order to investigate the role of the solid volume percentages of the substrate for the antenna performance, antennas were designed in three infill levels. Each antenna was comprised of a conductive patch and a ground mounted on a dielectric substrate (Fig. 2a). A 3 mm-thick TPU padding layer was included on top of the patch so as to avoid the direct contact between the breast phantom and the patch. In this configuration, the microwave radiation is achieved from the patch toward the center of the hemispheric breast tissue (Fig. 2b) (Mukai 2019; Mukai & Suh 2018, 2020). By computing the scattering (S)-parameter (S_{11}) with the dielectric property data on a 3D full-wave EM simulator (Ansys HFSS®), the antennas were designed to resonate at an industrial, scientific and medical (ISM) band (2.45 GHz).

The designed antennas were fabricated by 3D printing the TPU filament in the three infill percentages (100%, 70% and 40%) for the substrate, followed by mounting an adhesive-backed copper foil to constitute a radiating patch and a ground plane. To this structure, a 3 mm-thick 3D-printed TPU layer was placed for the padding purpose. While 100%- and 70%-infill samples (Fig. 3) were successfully printed, fabrication of the 40%-infill antenna was not satisfactory. Because of the high flexibility of the TPU material together with the highly porous (40%-infill) structure, it was not successful to achieve the hemispheric structure. The printed object was not firm enough and ended up slightly skewed to one direction. This involved the printed body being contacted by a printing nozzle at an undesirable contact point. Therefore, the final antenna simulation and fabrication only included the antennas printed with 70% and 100% solid infills.

Fig. 2 Patch antenna in **a** perspective and **b** cross-sectional views

Mukai *et al. Fash Text*   (2021) 8:24

Page 5 of 12

Fig. 3 Antenna sample (100%-infill): **a** ground plane side and **b** patch side

Fig. 4 Antenna powering setup for temperature measurement. Reprinted from (Mukai & Suh 2020)

Specific absorption rate calculation

The specific absorption rate (SAR) is the amount of EM energy absorbed per unit mass of tissue and is expressed as:

$$SAR = \frac{\sigma |E|^2}{\rho} \; (W/kg) \tag{1}$$

where σ is the conductivity (S/m) of the tissue; $|E|$ is the amplitude of the electric field (V/m); and is the tissue density (kg/m^3) (Ito et al. 2001). Thus, the SAR is equivalent to the amount of heat generated by the EM irradiation and can be used as a practical indicator of the heating efficacy of a hyperthermia device. The SAR was computed by running the EM simulator (Ansys HFSS$^®$). In the simulation, the input power was set to 1 W, and the SAR was plotted within the tissue-equivalent breast model irradiated by the 100%-infill and 70%-infill antennas.

Antenna measurements

To validate the antenna design, the reflection coefficient (S_{11}) was measued by the vector network analyzer in the frequency range of 1 to 3.5 GHz. The temperature of the breast phantom was monitored at two locations (5 mm and 7 mm from the apex of the phantom) by using thermocouple sensor probes conncected to a thermometer (Fluke 52 II Dual Probe Digital Thermometer). Following previous research (Mukai 2019; Mukai and Suh 2020), 30 dBm power at 2.45 GHz was supplied to the antenna sample by connecting a 10 dBm signal generator (SynthNV) and a 20 dB gain block (Sireen 2.4 GHz 1 W High Gain Amplifier Module) as shown in Fig. 4.

Table 1 Dielectric properties of 3D-printed TPU in three different infill levels

Infill (%)	Solid volume (%)	Dielectric constant	Loss factor
40.0	43.6	1.59	0.05
70.0	71.8	1.79	0.05
100.0	100.0	2.36	0.05

Fig. 5 Schematic of the 3D-printed TPU with shells used for dielectric characterization
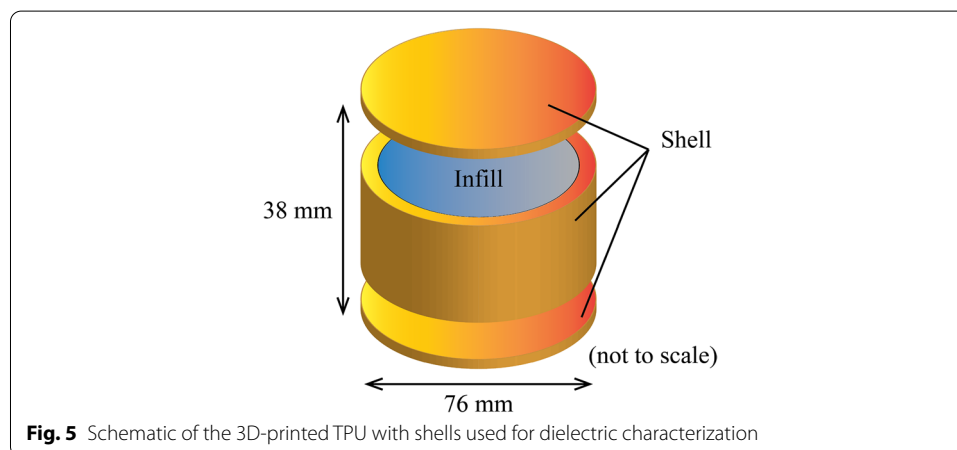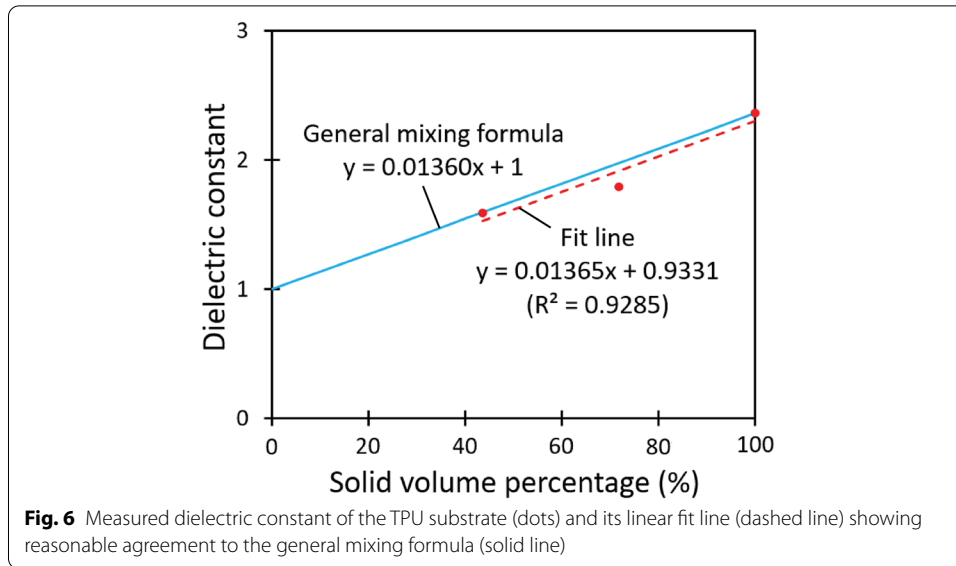
Results and discussion

Dielectric properties of TPU

Dielectric properties of the TPU substrates in the three different infill levels were successfully characterized and are given in Table 1. As depicted in Fig. 5, the 3D-printed TPU samples had shell layers, and hence the actual solid volume percentages were slightly higher than the infill percentages. While the loss factor remained unchanged, it was observed that with reduction in the solid volume percentage from 100% to 43.6%, the dielectric constant was lowered from 2.36 to 1.59. This relationship between the solid volume percentage (x) and the dielectric constant (y) was nearly linear ($y = 0.01365x + 0.9331$, $R^2 = 0.9285$) and in reasonable accordance with the classic mixing formula ($y = 0.01360x + 1$) (Bal & Kothari 2010; Tuncer et al. 2002) as plotted in Fig. 6. Hence, this observation led to a deduction that the dielectric constant is linearly related to the solid volume (infill) percentage and could be well-predicted by the existing formula.

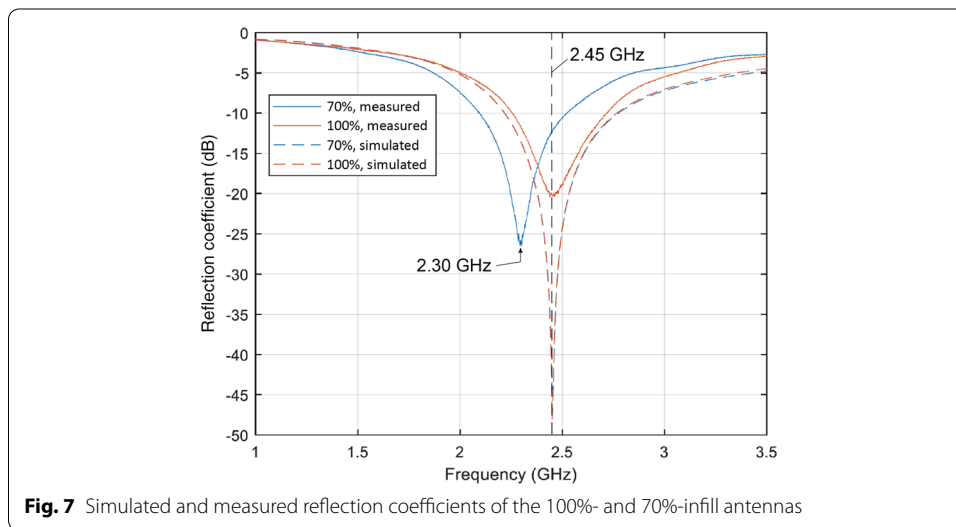### Optimal antenna dimensions and impedance matching

Table 2 shows the optimized dimensions of the antennas. In this optimization, the dielectric constant of 2.06 (obtained from the fit line, Fig. 6) was used for the 70%-infill antenna since the actual solid volume percentage of this antenna was 82.4% considering the shell layers. The 100%- and 70%-infill antennas had similar dimensions, but the patch length of the 70%-infill antenna was slightly longer than that of the 100%-infill antenna to compensate the smaller dielectric constant of the substrate.

Figure 7 gives the simulated and measured reflection coefficients (S_{11}) of the antennas. The simulation showed that both 100%- and 70%-infill antennas had resonance at 2.45 GHz with well-matched impedance (-48.1 dB and -44.2 dB), respectively. The

Mukai *et al. Fash Text*   (2021) 8:24

Page 7 of 12

Fig. 6 Measured dielectric constant of the TPU substrate (dots) and its linear fit line (dashed line) showing reasonable agreement to the general mixing formula (solid line)

Table 2 Dimensions of the antenna samples

Infill (%)	Solid volume (%)	Dielectric constant	Loss factor	Patch length (mm)	Patch width (mm)	Ground length (mm)	Ground width (mm)
70.0	82.4	2.06	0.05	39.8	19.4	76.4	76.4
100.0	100.0	2.36	0.05	37.8	19.4	76.4	76.4

Fig. 7 Simulated and measured reflection coefficients of the 100%- and 70%-infill antennas

measured reflection coefficient of the 100%-infill antenna sample was also matched reasonably (-20.3 dB) to 2.45 GHz, verifying the validity of the antenna design. However, the 70%-infill antenna sample exhibited a resonance at 2.30 GHz (-26.5 dB), instead of 2.45 GHz. While there could be several possibilities involved, the primary cause for this unexpected observation would be the flexural distortion. Comprised of a highly flexible
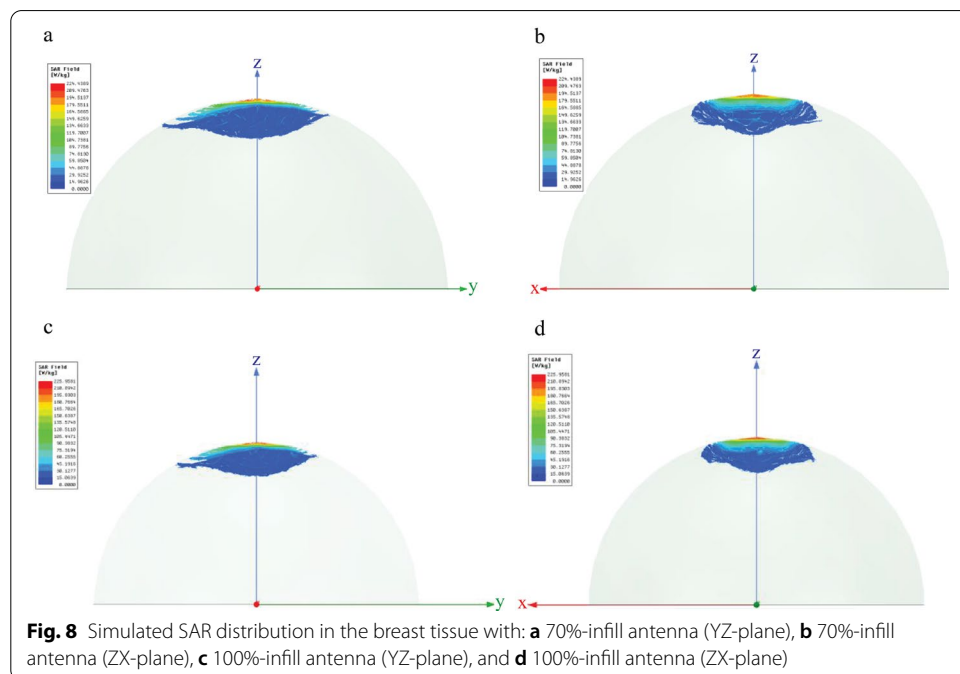
TPU with a relatively low (70%) infill, the substrate could have had a compressional distortion, leading to a decrease of the effective substrate thickness. Because a thinner substrate is known to incur a downshift in the resonant frequency (Balanis 2012, 2016), the lower resonant frequency of the 70%-infill antenna sample could be elucidated. Although there was a minor frequency shift with the 70%-infill antenna sample, this antenna still maintained a good reflection coefficient lower than −10 dB at 2.45 GHz, and therefore, it could be claimed that the antenna design was still valid from the impedance matching point of view.
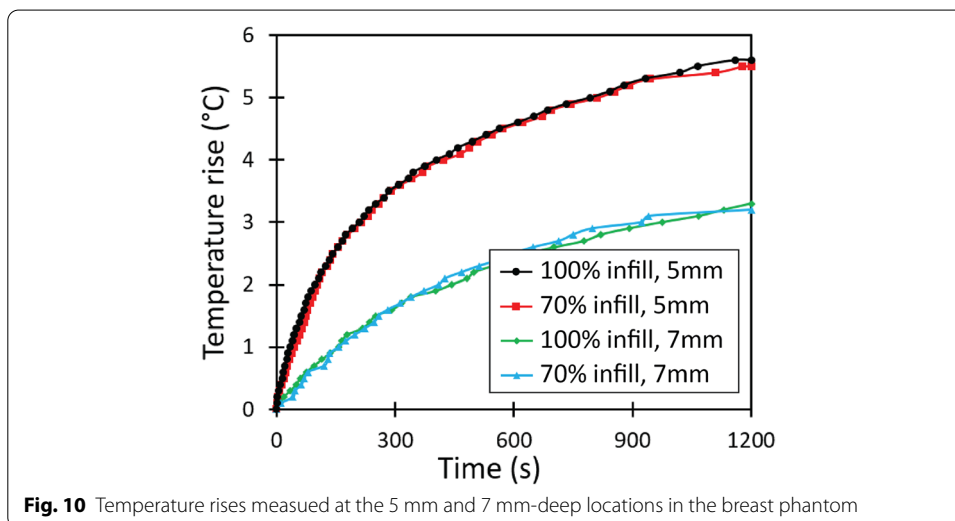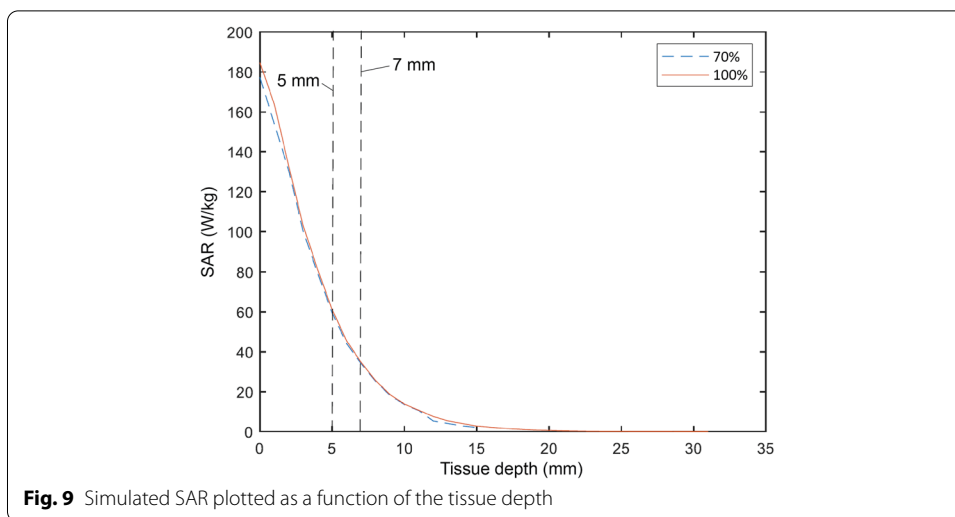
SAR distribution

Figure 8 shows the simulated SAR distribution in the breast phantom. Due to the highly lossy nature of the breast tissue, a substantial absorption was observed in the superficial areas of the tissue, with no significant difference between the antennas of different infill percentages. For both antennas, the SARs were ~60 W/kg and ~35 W/kg at the 5 mm- and 7 mm-deep tissues, respectively (Fig. 9). Although the SAR required in the actual treatment settings would be largely dependent on the various factors such as tumor size and blood perfusion pattern, according to some studies, the SARs ranging from 8 to 83 W/kg were necessary to maintain the temperature (Griffiths et al. 1986; Halac et al. 1983; Oleson et al. 1983). Therefore, the SARs acquired in this work could be sufficient for hyperthermia treatment.

The SARs simulated at different tissue depths (Fig. 9) indicated that there was no significant energy absorption in the locations deeper than ~15 mm. Microwaves hardly go beyond this depth, and this suggested that only a superficial treatment would be possible, as also reported as a major challenge in microwave hyperthermia in literature (Arce-Salinas et al. 2013; Bellon et al. 2016; Mukai 2019; Mukai & Suh 2020; Stauffer 2000).

Fig. 8 Simulated SAR distribution in the breast tissue with: **a** 70%-infill antenna (YZ-plane), **b** 70%-infill antenna (ZX-plane), **c** 100%-infill antenna (YZ-plane), and **d** 100%-infill antenna (ZX-plane)

Fig. 9 Simulated SAR plotted as a function of the tissue depth

Fig. 10 Temperature rises measued at the 5 mm and 7 mm-deep locations in the breast phantom

Temperature increment

The measured temperature rises are plotted in Fig. 10. There was little difference in the heating performance of the antennas with the substrate of different infill percentages, as the size of the radiating patch was optimized according to the dielectric properties of the substrate. This finding has an implication that antenna tuning is possible by precisely controlling substrate infill percentages in reverse.

The temperature rises were ~ 5.5 °C and ~ 3.2 °C at the tissue depths of 5 mm and 7 mm, respectively, after 20 min treatment (Table 3). This difference in the temperature rises in the two depths was most likely the consequence of the limited penetration of the applied microwaves as evidenced by the SAR simulation results (Fig. 9). Although the treatment would be limited to superficial regions, these findings support the possibility of administering hyperthermia therapy with the 3D-printed antennas.

Table 3 Measured temperature rises after 20 min of heating

Infill (%)	Solid volume (%)	Temperature rise (°C) at 5 mm	Temperature rise (°C) at 7 mm
70.0	82.4	5.5	3.2
100.0	100.0	5.6	3.3

Conclusions

This paper presented the design, fabrication and characterization of a 3D-printed TPU antenna for microwave hyperthermia applications. By using the resonant cavity method, the dielectric properties of TPU substrates were successfully characterized in three levels of infill percentages. It was found that the dielectric constant increased almost linearly with the solid volume percentage, and this was well supported by the general theory of dielectric mixtures reported in literature. On the other hand, the loss factor was independent of the solid volume percentages under the resolution of the resonant cavity measurements.

Based on the characterized dielectric properties, the antennas were designed in three infill levels and fabricated in the optimal geometry and dimensions. However, the antenna with the lowest infill percentage was excessively vacant to self-maintain its structure. Accordingly, further experiments were continued with antennas in the higher infill percentages.

The SARs of the antennas were calculated with a homogeneous breast model under an input power of 1 W. It was found that the most absorption occurred in the superficial areas (less than 15 mm from the apex) due to the highly lossy composition of the breast. The limited penetration of microwave was confirmed by measurements: for both antenna samples of different infill levels, the measured temperature rises at 5 mm and 7 mm locations were respectively ∼ 5.5 °C and ∼ 3.2 °C after 20 min of continuous irradiation. The variation in dielectric constants was successfully controlled by antenna designs and did not critically cause consequent difference in heating efficacy. Although the treatment depth would be limited to the near-surface region, the current data support the possibility of administering hyperthermia treatment with the 3D-printed TPU antenna.

Limitations and recommendations

Although this work sheds light on the prospect of breast hyperthermia with 3D-printed flexible antennas, there are a couple of limitations to be noted. First, the antenna samples developed in this work contained adhesive-backed copper foils to constitute a patch and a ground. While an initial attempt was made to 3D print an electrically conductive filament (Electrifi, Multi3D, LLC) as the patch and ground plane, the resulting conductivity of the prints was not sufficient for the hyperthermia antenna application (Li 2019). For this reason, the copper foil was employed in this work. In order to realize truly 3D printable and seamlessly manufacturable antennas, a future work is recommended to incorporate a flexible filament with superior electrical properties.

Secondly, the results and conclusions of this paper should not directly apply to the case of in-vivo tissues. The employed breast phantom was homogeneous and did not precisely mimic the actual biophysical representation of the human body. There are innumerable components in real female breasts. Those include skin, fats, benign and malignant tumors and blood vessels of a variety of dielectric, electrical and thermal properties, all of which could influence the heating efficacy. For a further study, it is thus indispensable to consider a more realistic phantom.

Availability of data and materials
The datasets used and analyzed during the current study are available from the corresponding author on reasonable request.

Competing interests
The authors declare that there are no competing interests.

Author details
[1] Department of Textile Engineering, Chemistry and Science, North Carolina State University, Raleigh, NC, USA.
[2] Associate Professor, Department of Textile and Apparel, Technology and Management, North Carolina State University, 1020 Main Campus Drive, Raleigh, NC 27606, USA.

References
Anghileri, L. J., & Robert, J. (2019). *Hyperthermia in cancer treatment*. Boca Raton: CRC Press.
Arce-Salinas, C., de la Garza-Salazar, J. G., & Meneses García, A. (2013). *Inflammatory breast cancer*. Berlin: Springer.
Bal, K., & Kothari, V. K. (2010). Permittivity of woven fabrics: A comparison of dielectric formulas for air-fiber mixture. *IEEE Transactions on Dielectrics and Electrical Insulation, 17*(3), 881–889. https://doi.org/10.1109/TDEI.2010.5492262.
Balanis, C. A. (2012). *Advanced engineering electromagnetics* (2nd ed.). New York: Wiley.
Balanis, C. A. (2016). *Antenna theory: Analysis and design* (4th ed.). New York: Wiley.
Bellon, J. R., Wong, J. S., MacDonald, S. M., & Ho, A. Y. (2016). *Radiation therapy techniques and treatment planning for breast cancer*. Berlin: Springer.
Bharambe, V. T. (2016). *Analysis of liquid metal vacuum filling approach to develop 3D printed antenna* [Unpublished master's thesis]. North Carolina State University.
Bjorgaard, J., Hoyack, M., Huber, E., Mirzaee, M., Chang, Y.-H., & Noghanian, S. (2018). Design and fabrication of antennas using 3D printing. *Progress in Electromagnetics Research C, 84,* 119–134. https://doi.org/10.2528/PIERC18011013.
Curto, S., & Prakash, P. (2015). Design of a compact antenna with flared groundplane for a wearable breast hyperthermia system. *International Journal of Hyperthermia, 31*(7), 726–736. https://doi.org/10.3109/02656736.2015.1063170.
Curto, S., Ramasamy, M., Suh, M., & Prakash, P. (2015). Design and analysis of a conformal patch antenna for a wearable breast hyperthermia treatment system. *Energy-Based Treatment of Tissue and Assessment VIII, 9326,* 93260l. https://doi.org/10.1117/12.2079718.
Curto, S., Garcia-Miquel, A., Suh, M., Vidal, N., Lopez-Villegas, J. M., & Prakash, P. (2018). Design and characterisation of a phased antenna array for intact breast hyperthermia. *International Journal of Hyperthermia, 34*(3), 250–260. https://doi.org/10.1080/02656736.2017.1337935.
Griffiths, H., Ahmed, A., Smith, C. W., Moore, J. L., Kerby, I. J., & Davies, R. M. E. (1986). Specific absorption rate and tissue temperature in local hyperthermia. *International Journal of Radiation Oncology Biology Physics, 12*(11), 1997–2002. https://doi.org/10.1016/0360-3016(86)90137-9.
Halac, S., Roemer, R. B., Oleson, J. R., & Cetas, T. C. (1983). Uniform regional heating of the lower trunk: Numerical evaluation of tumor temperature distributions. *International Journal of Radiation Oncology Biology Physics, 9*(12), 1833–1840. https://doi.org/10.1016/0360-3016(83)90351-6.
Ito, K., Furuya, K., Okano, Y., & Hamada, L. (2001). Development and characteristics of a biological tissue-equivalent phantom for microwaves. *Electronics and Communications in Japan Part I Communications, 84*(4), 67–77. https://doi.org/10.1002/1520-6424(200104)84:4%3c67::AID-ECJA8%3e3.0.CO;2-D.
Li, S. (2019). *3D-printed conformal antennas for wearable hyperthermia device* [Unpublisehd master's thesis]. North Carolina State University.

Liang, M., Wu, J., Yu, X., & Xin, H. (2016). *3*D printing technology for RF and THz antennas. *2016 international symposium on antennas and propagation (ISAP), Japan,* 536-537. https://ieeexplore.ieee.org/document/7821190

Locher, I., Klemm, M., Kirstein, T., & Trster, G. (2006). Design and characterization of purely textile patch antennas. *IEEE Transactions on Advanced Packaging, 29*(4), 777–788. https://doi.org/10.1109/TADVP.2006.884780.

Mirzaee, M., Noghanian, S., Wiest, L., & Chang, I. (2015). Developing flexible 3D printed antenna using conductive ABS materials. *2015 IEEE international symposium on antennas and propagation & USNC/URSI national radio science meeting, Canada,* 1308–1309. https://doi.org/10.1109/APS.2015.7305043

Mukai, Y. (2016). *Inkjet-printed wearable antennas for hyperthermia treatment* [Unpublished master's thesis]. North Carolina State University.

Mukai, Y. (2019). *Dielectric properties of cotton fabrics and their applications* [Unpublished doctoral dissertation]. North Carolina State University.

Mukai, Y., Bharambe, V. T., Adams, J. J., & Suh, M. (2018). Effect of bending and padding on the electromagnetic performance of a laser-cut fabric patch antenna. *Textile Research Journal, 89*(14), 2789–2801. https://doi.org/10.1177/0040517518801202.

Mukai, Y., Dickey, E. C., & Suh, M. (2020). Low frequency dielectric properties related to structure of cotton fabrics. *IEEE Transactions on Dielectrics and Electrical Insulation, 27*(1), 291–298. https://doi.org/10.1109/TDEI.2019.008511.

Mukai, Y., & Suh, M. (2018). Development of a conformal textile antenna for thermotherapy. *Fiber society's fall 2018 technical meeting and conference, USA.* https://www.thefibersociety.org/Portals/0/Past%20Conferences/2018_Fall_Abstracts.pdf?ver=2019-01-22-095426-997

Mukai, Y., & Suh, M. (2019a). Structure-microwave dielectric property relationship in cotton fabrics. *Techtextil North America, USA.*

Mukai, Y., & Suh, M. (2019b). Conformal cotton antenna for wearable thermotherapy. *Fiber Society's Spring 2019 Conference, Hong Kong.* http://thefibersociety.org/Portals/0/Past%20Conferences/2019_Spring_Abstracts.pdf?ver=2019-07-16-122240-037

Mukai, Y., & Suh, M. (2020). Development of a conformal polyester fabric antenna for wearable breast hyperthermia. *Fashion & Textiles, 6,* 062001.

Noorani, R. (2017). *3D printing: Technology, applications, and selection*. Boca Raton: CRC Press. https://doi.org/10.1201/9781315155494.

Oleson, J. R., Heusinkveld, R. S., & Manning, M. R. (1983). Hyperthermia by magnetic induction: II. Clinical experience with concentric electrodes. *International Journal of Radiation Oncology Biology Physics, 9*(4), 549–556. https://doi.org/10.1016/0360-3016(83)90074-3.

Pang, L., & Lee, K. (2016). *Hyperthermia in oncology*. Boca Raton: CRC Press.

Peng, S., Zeng, Q., Yang, X., Hu, J., Qiu, X., & He, J. (2016). Local dielectric property detection of the interface between nanoparticle and polymer in nanocomposite dielectrics. *Scientific Reports, 6,* 38978. https://doi.org/10.1038/srep38978.

Ramasamy, M., Curto, S., Prakash, P., & Suh, M. (2015). Conformable antenna development for wearable hyperthermia device. The fiber society 2015 fall meeting and technical conference*, USA.* http://thefibersociety.org/Portals/0/Past%20Conferences/2015_Fall_Abstracts.pdf

Stauffer, P. R. (2000). *T*hermal therapy techniques for skin and superficial tissue disease. *Matching the energy source to the clinical need: a critical review, USA,102970*, 102970E. https://doi.org/10.1117/12.375215

Tuncer, E., Serdyuk, Y. V., & Gubanski, S. M. (2002). Dielectric mixtures: Electrical properties and modeling. *IEEE Transactions on Dielectrics and Electrical Insulation, 9*(5), 809–828. https://doi.org/10.1109/TDEI.2002.1038664.

Xu, F., Zhang, K., & Qiu, Y. (2020). Light-weight, high-gain three-dimensional textile structural composite antenna. *Composites Part B: Engineering, 185,* 107781. https://doi.org/10.1016/j.compositesb.2020.107781.

Zajicek, R., & Vrba, J. (2010). Broadband complex permittivity determination for biomedical applications. In V. Zhurbenko (Ed.), *Advanced microwave circuits and systems* (pp. 365–386). IntechOpen: Rijeka.

Publisher's Note
Springer Nature remains neutral with regard to jurisdictional claims in published maps and institutional affiliations.